



MATHEMATICAL MODEL OF WARM DRAWING OF MgCa0.8 ALLOY ACCOUNTING FOR DUCTILITY OF THE MATERIAL

ANDRZEJ MILENIN *, PIOTR KUSTRA, MAREK PAĆKO

AGH University of Science And Technology, Krakow, Poland

**Corresponding Author: milenin@agh.edu.pl*

Abstract

The results of experimental and numerical analysis of MgCa0.8 magnesium alloy are presented in the paper. Basing on experimental tests the flow stress function and the dependencies between ductility strain, triaxiality factor, temperature and strain rate were obtained. Experiment was performed on the testing machine Zwick Z250. The algorithm based on the inverse method was used to interpret correctly experimental results. The FEM modelling of upsetting and tension tests was helpful to obtain conditions of material fracture. The developed models of mechanical properties were implemented into the Drawing2d FEM code and simulations of drawing of surgical threads were performed. The introduced approach enabled modelling of the drawing process at elevated temperatures, accounting for the material fracture.

Key words: MgCa0.8 alloy, wire drawing, FEM, surgical threads

1. INTRODUCTION

Magnesium alloys are more often used in aerospace, automotive, electronics etc. industries. These alloys are formed similarly to other metals, using processes of rolling, forging, extrusion, stamping and many other technological processes applicable at elevated temperatures (Watanebe et al., 2004; Ogawa et al., 2002; Swiostek et al., 2006; Cheng, et al., 2007). Performed studies by Bach et al.'s (2006), Heublein et al.'s (1999); Haferkamp et al.'s (2001), Wan et al.'s (2008) have shown that by certain improvement of the chemical composition (usually adding a small amount of Ca, Li), magnesium alloys achieve a high level of biocompatibility with the human body and dissolve in the body without significant medical problems. Several new magnesium alloys for biomedical applications (such as MgCa, LAE442, MgCa0.8) were developed at the University of Hanover (Bach et al., 2006; Thomann et al.,

2008). Production of surgical threads to integration of tissue can be an example of application of these types of alloys. These applications requires fine wires with diameters from 0.1 mm to 0.9 mm. Due to poor formability and limited ductility of magnesium alloys in room temperature, drawing process to dimension 0.1 mm is difficult.

Low ductility of the magnesium alloys corresponds to their hexagonal close packed structure. Thus, the process of cold forming is practically impossible (Eickemeyer et al., 2004). Von Misses (1928) writes that the plastic deformation needs minimum of 5 independent slip systems. In the case of magnesium alloys at room temperature there are only 3 independent slip systems. Therefore, it is necessary to increase the number of slip systems, for instance by raising the temperature. In Bach et al.'s work (2005) a new manufacturing technology of tubes made of Mg alloys is proposed. In this technology the metal is heated by a hot die and the proc-

ess of warm deformation is performed. The theoretical description of the wire drawing process with a heated die is presented by Bach et al. (2007) and Milenin and Kustra (2008).

The model of material ductility is a very important part of the FE program for simulation of drawing. Availability of this model enables optimization of the process of wire drawing on the basis of the FE simulations. Fracture problems for magnesium alloys are precisely described in literature (Eickemeyer et al., 2004; Milenin & Kustra, 2008; Yoshida, 2004). However, these works account for only few parameters of drawing, such as the die angle and the reduction ratio. Magnesium alloys containing aluminum and zinc (such as AZ31) are investigated materials, which have a bigger plasticity than Mg-Ca alloys. However, the ductility models of Mg-Ca alloys are scarce in the literature. The yield stress models of the latter alloy for warm deformation are not available in the literature, either.

The purpose of this paper is the development of mathematical models of the yield stress and the ductility for the MgCa0.8 alloy, implementation of these models into the FE code and simulations of wire drawing processes in heated die.

2. FEM MODEL OF PLASTIC DEFORMATION IN DRAWING

The FE code Drawing2d developed by Milenin (2005) is used in the present work. The FE model solves a boundary problem considering such phenomena as metal deformation, heat transfer in a die and in a wire, metal heating due to deformation and friction. Solution of the boundary problem is obtained by using variation principle of rigid-plastic theory:

$$J = \int_V \int_0^{\xi_i} \sigma_s(\varepsilon_i, \xi_i, t) d\xi_i dV + \int_V \sigma_0 \xi_0 dV - \int_S \sigma_\tau v_\tau dS, \quad (1)$$

where: ξ_i – strain rate, σ_s – yield stress, ε_i – effective strain, t – temperature, V – volume, σ_0 – mean stress, ξ_0 – volumetric strain rate; S – contact area between alloy and die, σ_τ – friction stress, v_τ – alloy slip velocity along area of die.

The friction stress is determined according to law:

$$\sigma_\tau = f_{tr} \frac{\sigma_s}{\sqrt{3}} \left[1 - \exp\left(-\frac{1.25\sigma_n}{\sigma_s}\right) \right], \quad (2)$$

where: f_{tr} – friction coefficient, σ_n – normal stress on contact between the deformed alloy and the die.

The stress tensor σ_{ij} is calculated on the basis of the strain rate tensor ξ_{ij} according to the following equation:

$$\sigma_{ij} = \delta_{ij} \sigma_0 + \frac{2\sigma_s}{3\xi_i} \xi_{ij}. \quad (3)$$

The stationary formulation of this task is used in the paper. The tensor ε_{ij} is calculated by integration along the flow lines:

$$\varepsilon_{ij} = \int_0^\tau \xi_{ij}(\tau) d\tau = \sum_{p=1}^{p=p_\tau} \xi_{ij}^{(p)} \Delta\tau^{(p)}, \quad (4)$$

where: $\Delta\tau^{(p)}$ – time increment, $\xi_{ij}^{(p)}$ – strain rate tensor determined according to equation:

$$\xi_{ij}^{(p)} = \sum_{n=1}^{n_{nd}} N_n \xi_{ijn}, \quad (5)$$

where: N – finite element shape functions, ξ_{ijn} – nodal strain rate tensor for current finite element, n_{nd} – number of nodes in element.

The points of flow lines are determined on the basis of the values of the velocity at the point p , which are calculated according to the following formula:

$$v_i^{(p)} = \sum_{n=1}^{n_{nd}} N_n v_{in}. \quad (6)$$

The calculation of the position of the next point ($p+1$) of flow line is carried out according to the equation:

$$x_i^{(p+1)} = x_i^{(p)} + v_i^{(p)} \Delta\tau. \quad (7)$$

3. THE FEM SOLUTION OF THE THERMAL PROBLEM IN METAL

Thermal problem is solved by applying the following method. The passage of the section through the zone of deformation is simulated. For this section at each time step the non-stationary temperature problem is examined:

$$\lambda \left(\frac{\partial^2 t}{\partial r^2} + \frac{1}{r} \frac{\partial t}{\partial r} \right) + Q_d = c\rho \frac{dt}{d\tau} \quad (8)$$



where: $Q_d = 0.9\sigma_s \dot{\xi}_i$ – deformation power, c – specific heat; ρ – alloy density, τ – time, λ – thermal conductivity coefficient (the following values are used for MgCa0.8 alloy: $c = 624$ J/kgK, $\rho = 1738$ kg/m³, $\lambda = 126$ J/mK), r – y cylindrical coordinates. Heat exchange between the alloy and the die is defined as:

$$q_{conv} = \alpha(t - t_{die}) \quad (9)$$

where: t_{die} – die temperature, α – heat exchange coefficient.

The generation of heat from friction is calculated according to the formula:

$$q_{fr} = 0.9\sigma_\tau v_\tau. \quad (10)$$

4. FEM SOLUTION OF THERMAL PROBLEM IN THE DIE

The model of temperature distribution in the die is based on the solution of Fourier equation in the cylindrical coordinate system:

$$\lambda \left(\frac{\partial^2 t}{\partial r^2} + \frac{1}{r} \frac{\partial t}{\partial r} + \frac{\partial^2 t}{\partial y^2} \right) + Q_h = 0 \quad (11)$$

where: Q_h – power of the heating element.

The heat Q_h is generated in the finite elements, which correspond to the position of heating device. The boundary problem is solved on the basis of the variation formulation of equation (11). For the areas, which are in contact with the metal, the temperature of the alloy is obtained from the solution of the thermal problem for the metal.

5. DUCTILITY MODEL

The key parameter, which presents fracture, was named ductility function. This parameter is determined by the following formula:

$$\psi = \frac{\xi_i}{\varepsilon_p(k, t, \xi_i)} < 1, \quad (12)$$

where: k – triaxiality factor, $k = \sigma_0 / \sigma_s$.

Critical deformation function $\varepsilon_p(k, t, \xi_i)$ is obtained and is based on experimental studies. In the Drawing2d FEM code equation (12) was implemented as a following integral:

$$\psi = \int_0^\tau \frac{\xi_i}{\varepsilon_p(k, t, \xi_i)} d\tau \approx \sum_{m=1}^{m=m_i} \frac{\xi_i^{(m)}}{\varepsilon_p(k, t, \xi_i)} \Delta\tau^{(m)}, \quad (13)$$

where: τ – time of deformation, $\Delta\tau^{(m)}$ – current time increment, $\xi_i^{(m)}$ – values of the strain rate in the current time, m – index number of time step during numerical integration along the flow line.

Critical deformation function $\varepsilon_p(k, t, \xi_i)$ can be obtained on the basis of experimental results for the upsetting and tension tests at different values of k, t, ξ_i .

6. EXPERIMENTAL STUDIES

MgCa0.8 magnesium alloy was used as a testing material. Figure 1 shows the dimensions and shape of samples for upsetting and tensile tests. Upsetting tests were used to determine the flow stress model. Both upsetting and tensile tests were used to calculate coefficients of critical deformation function. The material tests were performed in a Zwick Z250 testing machine at the AGH University of Science and Technology in Krakow, Poland. Results and conditions of all the tests are presented in tables 1 and 2. The range of temperature and strain rate changes in the experiments was selected in accordance with the conditions for the deformation of metal during wire drawing in the heated dies.

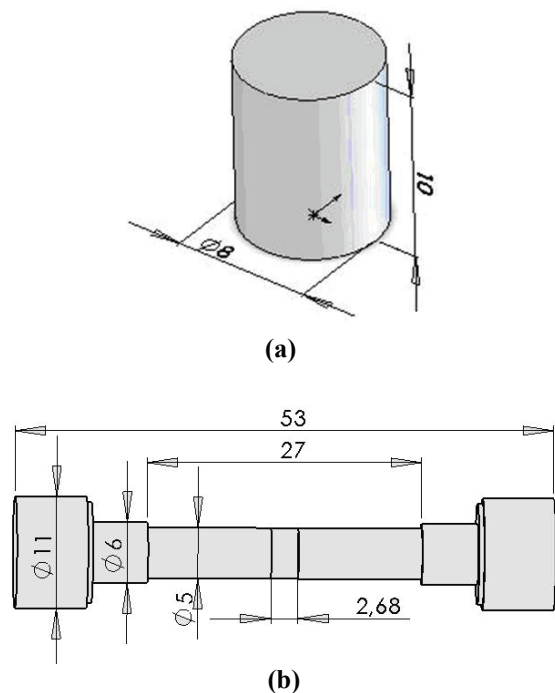


Fig. 1. Shape and dimension of samples for upsetting test (a) and tensile test (b).



7. YIELD STRESS MODEL

Yield stress model σ_s for analyzed alloys was proposed as a modified Hansel-Spittel equation:

$$\sigma_s = A \exp(-m_1 t) \varepsilon_i^{m_2} \xi_i^{m_3} \left(\frac{t-20}{280}\right)^{m_6} \exp\left(\frac{m_4}{\varepsilon_i}\right) (1 + \varepsilon_i)^{m_5 t} \exp(m_7 \varepsilon_i) \xi_i^{m_8 t} t^{m_9}, \quad (14)$$

where: A, m_1-m_9 – empirical coefficients.

Experiment shows that σ_s is independent of the strain rate in low temperature (below 200°C), consequently, the expression $\left(\frac{t-20}{280}\right)^{m_6}$ was added to equation (14).

Table 1. Conditions and results of upsetting tests of MgCa0.8.

| Test Nr. | $t, ^\circ\text{C}$ | $v, \text{mm/min}$ | dH, mm | Critical deformation | k | Strain rate, 1/s | Shape of samples after tests |
|----------|---------------------|--------------------|-----------------|----------------------|-------|------------------|------------------------------|
| 1 | 300 | 60 | 5.8 | 1.3* (without crack) | -0.68 | 0.49 | |
| 2 | 300 | 600 | 5.6 | 1.2* (without crack) | -0.72 | 4.43 | |
| 3 | 250 | 60 | 6.1 | 1.8 | -1.13 | 0.58 | |
| 4 | 250 | 600 | 4.7 | 0.96 | -0.61 | 3.7 | |
| 5 | 200 | 60 | 3.0 | 0.45 | -0.51 | 0.22 | |
| 6 | 200 | 600 | 2.3 | 0.31 | -0.51 | 1.7 | |
| 7 | 100 | 60 | 1.8 | 0.23 | -0.47 | 0.15 | |
| 8 | 20 | 10 | 1.5 | 0.085 | -0.40 | 0.021 | |

*The destruction of the sample did not occur.

The coefficients in equation (14) were determined using the inverse approach (Szeliga & Pietrzyk, 2007) with the least squares method. The objective function was formulated as the root-mean-square difference between experimental and predicted loads. In the machine Zwick Z250 samples are heated together with the deforming tool. Consequently, the value of the gradient of the temperature in the model is insignificant. It makes possible to use

an engineering model of the process of upsetting in the inverse analysis. Results of this analysis are shown in figure 2. A relative error in the objective function was 0.055. The values of coefficients of equation (14) are presented in table 3. Plots of relation (14) for different temperatures and strain rates are shown in figure 3.

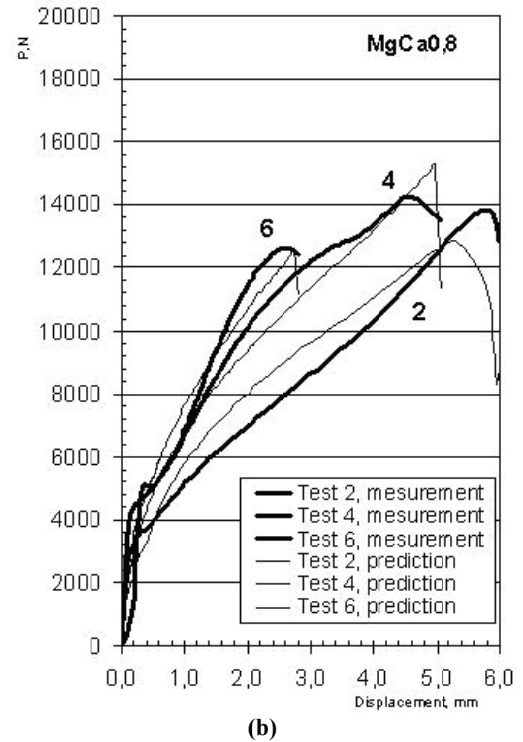
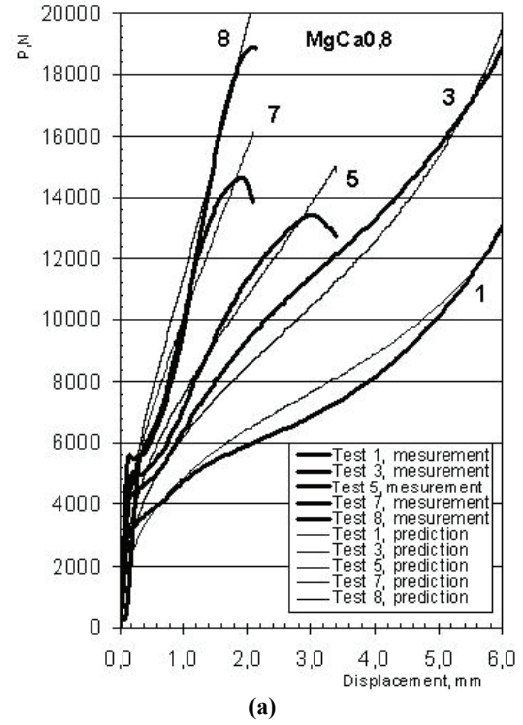


Fig. 2. Force versus displacement of the tool (deformation of the sample) in upsetting test: (a) test number 1,3,5,7,8 from table 1; (b) test number 2,4,6 from table 1, (thin line – modeling, thick line – experiment).



Table 2. Conditions and results of tensile tests of MgCa0.8.

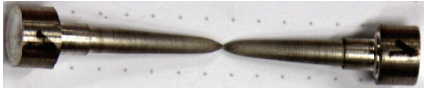
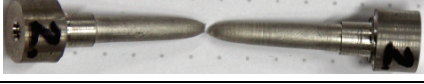



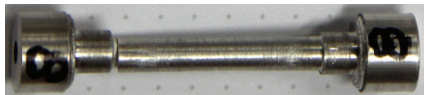
| Test Nr. | T, °C | V, mm/min | dL, mm | Critical deformation strain | Strain rate, 1/s | k | Shape of samples after tests |
|----------|-------|-----------|--------|-----------------------------|------------------|------|--|
| 1 | 300 | 60 | 22.5 | 3.8 | 0.60 | 0.85 |  |
| 2 | 300 | 600 | 16 | 2.38 | 5.4 | 0.45 |  |
| 3 | 250 | 60 | 14 | 0.76 | 0.11 | 0.45 |  |
| 4 | 250 | 600 | 8.5 | 0.41 | 0.66 | 0.34 |  |
| 5 | 200 | 60 | 7.5 | 0.32 | 0.041 | 0.34 |  |
| 8 | 20 | 10 | 1.55 | 0.065 | 0.0067 | 0.35 |  |

Table 3. Coefficients of yield stress equation (14)

| A | m ₁ | m ₂ | m ₃ | m ₄ | m ₅ | m ₆ | m ₇ | m ₈ | m ₉ |
|-------|----------------|----------------|----------------|----------------|----------------|----------------|----------------|----------------|----------------|
| 447.4 | 0.0007542 | 0.4485 | 0.2867 | -0.0001899 | -0.009392 | 2 | 0.8318 | -0.0004359 | 0.007962 |

8. CRITICAL DEFORMATION FUNCTION

Data in table 1 and 2 shows that critical deformation is dependent on the temperature, strain rate and value of k coefficient (in upsetting tests critical deformation is higher, than in tensile tests). Due to this fact the following relationship is proposed as a function of strain limit:

$$\varepsilon_p = d_1 \exp(-d_2 k) \exp(d_3 t) \xi_i^{d_4}, \quad (15)$$

where: $d_1 - d_4$ – empirical coefficients.

The following algorithm is proposed to calculate parameters of equation (15):

1. Using Forge software the numerical simulations of all experimental tests have been performed. Flow stress model was implemented in the form of equation (14) and the coefficients from table 3 were adopted.

2. Performed numerical modeling of all tests (upsetting and tensile) to determine changes in temperature, strain rate and k coefficient from the beginning of the test until the material cracking in the experiment.

3. Basing on the analysis of samples, the location of crack initiation was found. For upsetting tests it was observed that crack nucleation takes place in a corner of the sample (figure 4 (b)), while the tensile cracking begins in the axis of the sample. Reading of the process data from FEM models of tests was done in these points, which correspond to the location of the formation of the material crack. Example of results of the calculations are shown in figures. 4 - 5 for the test number 3 from table 1 and figures. 6-7 for the test number 1 in table 2. In the upsetting tests number 1 and 2 crack was not initiated, so this data was used only to verify the model (developed model (15) should give for those experiments $\psi < 1$).



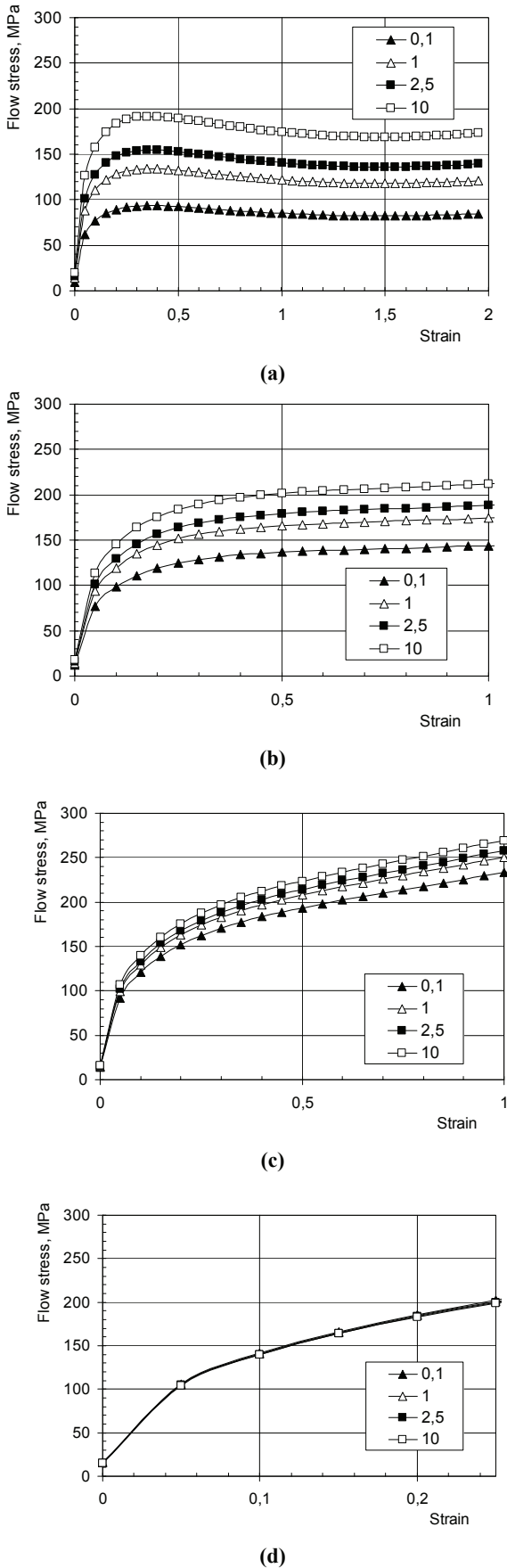


Fig. 3. Stress strain curves of MgCa0.8 magnesium alloy for temperatures (a) – 300 °C, (b) – 250 °C, (c) – 200 °C, (d) – 150 °C and strain rates 0.1, 1.0, 2.5 and 10 s⁻¹.

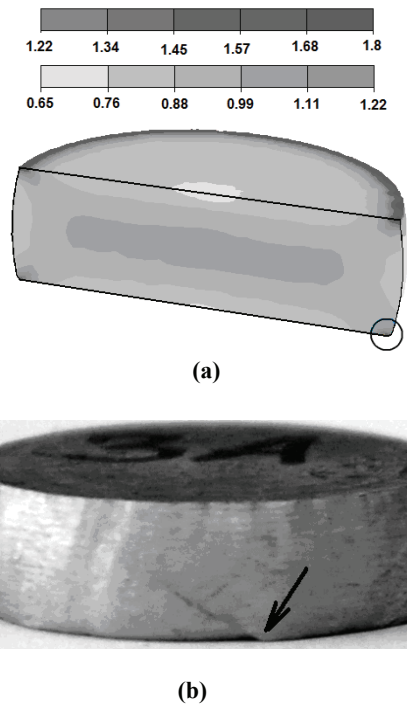


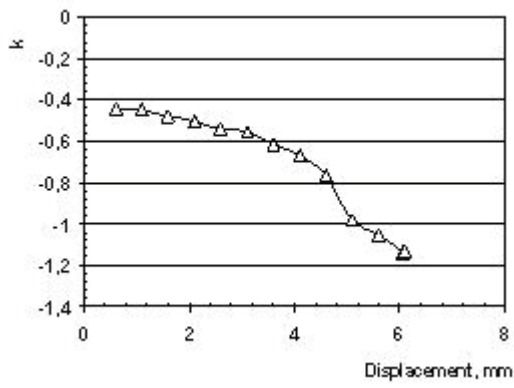
Fig. 4. Simulation result: distribution of effective strain for test 3 from table 1 (a), shape of the sample after the test 3 with marked location of crack (b).

4. The sets of parameter k , strain rate and temperature of the tensile and compression tests were used to develop coefficients $d_1 - d_4$ of the function (15). Coefficients were calculated using the least squares method. Change of ψ was described by equation (13). The sum of squares of difference between ψ_m^{calc} and 1.0 for strain, which corresponds to the crack observed in the experiment, was used as a goal function for the current test:

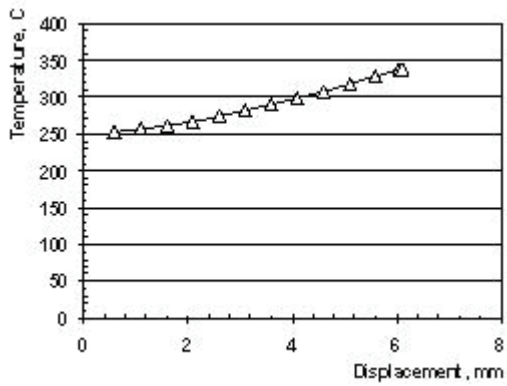
$$\delta = \sum_m^{m_{test}} (\psi_m^{calc} - 1)^2 \quad (16)$$

In the process of minimization of the function (16) the following parameters of equation (15) were obtained: $d_1 = 0.01530$; $d_2 = 0.1287$; $d_3 = 0.01575$; $d_4 = -0.2353$. The average relative error of approximation is 0.04. The dependences of critical deformation function on the strain rate and temperature are shown in figure 8.

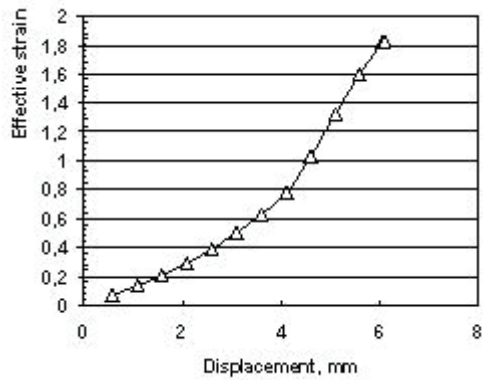




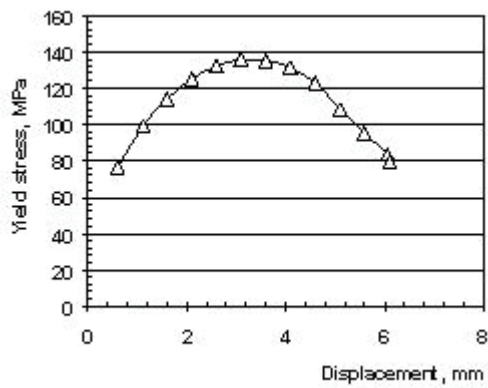
(a)



(b)

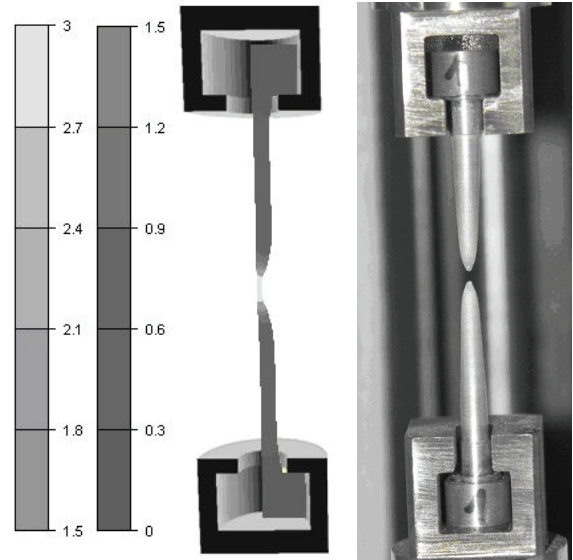


(c)



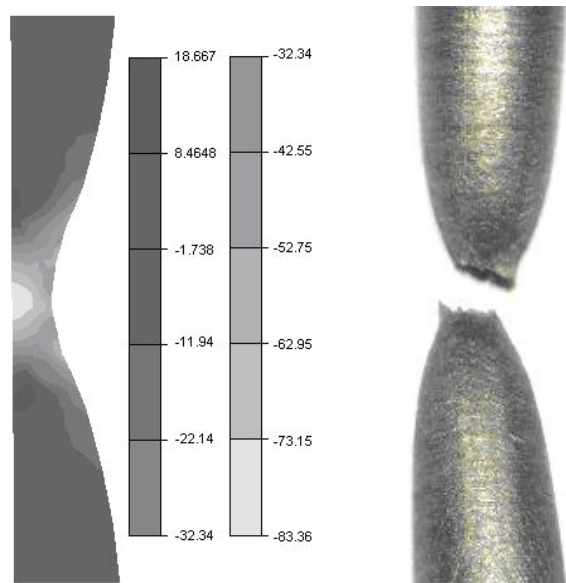
(d)

Fig. 5. The result of simulation the test number 3 from table 1 for the area marked in fig 4(a): (a) – change of the value k, (b) – temperature, (c) – effective strain and (d) – yield stress.



(a)

(b)



(c)

(d)

Fig. 6. The result of simulation of the test number 1 from table 2: distribution of effective strain (a), shape of sample after test (b), distribution of the main stress (c) and shape of the sample neck after the test (d).



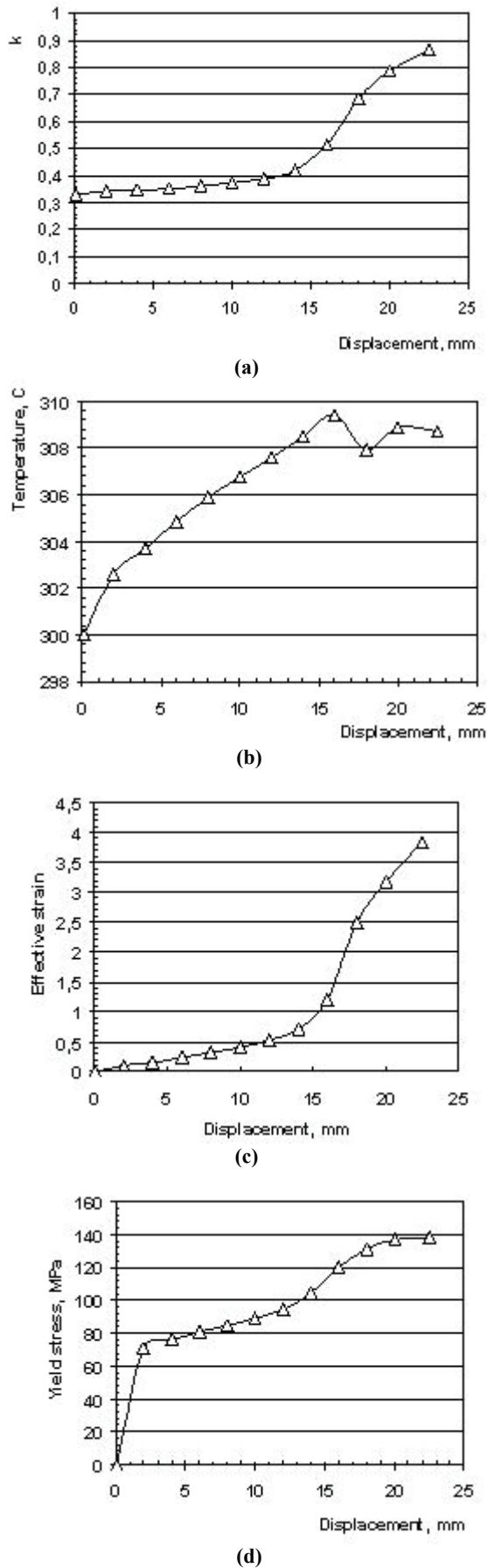


Fig. 7. The result of simulation of the test number 1 from table 2 for the center point of the sample: (a) – change in the value k , (b) – temperature, (c) – effective strain and (d) – yield stress.

9. ANALYSIS OF THE WIRE DRAWING PROCESS

Developed models of the flow stress (14) and the ductility (15) were implemented into the Drawing2d software. For the analysis of damage of the material three variants of drawing process were analyzed. General data given for all 3 variants (common data) are: coefficient of heat exchange with the environment $4000 \text{ W/m}^2\text{C}$; die temperature $t_c = 350^\circ\text{C}$, the temperature of the wire at the entrance to the valley of strain $t_0 = 100^\circ\text{C}$; initial wire diameter $d_0 = 0.5 \text{ mm}$, drawing angle $\alpha = 4^\circ$; length of the calibration part of die $L_2 = 0.1 \text{ mm}$; radius of the transition from the conical part of the calibration $r = 0.05 \text{ mm}$, coefficient of friction $f = 0.03$; drawing angle $\alpha = 4^\circ$.

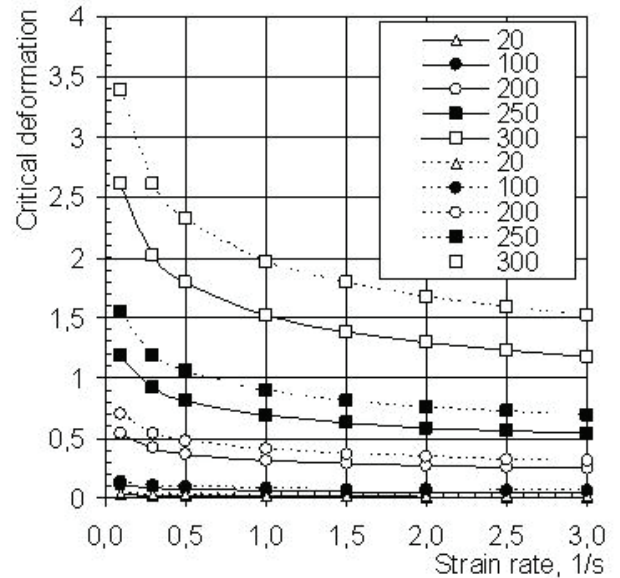


Fig. 8. Dependence of the critical deformation function on the effective strain for $k = -0.33$ (dotted line) and $k = 0.33$ (solid line) in temperatures 20°C , 100°C , 200°C , 250°C and 300°C .

The following numerical analyses were performed:

- Variant 1. Final diameter $d_1 = 0.38 \text{ mm}$; $v = 0.05 \text{ m/s}$;
- Variant 2. Final diameter $d_1 = 0.46 \text{ mm}$; $v = 0.05 \text{ m/s}$;
- Variant 3. Final diameter $d_1 = 0.46 \text{ mm}$; $v = 0.02 \text{ m/s}$.

The simulation results are shown in figure 9. Variant 1 corresponds to the elongation factor 1.73. The experimental knowledge based on drawing of Mg alloys shows that with such a large elongation factor, a break of the wire should be observed. The analysis of strain distribution (figure 9a) makes it possible to assert that the deformation is localized in the place of the application of force of wire drawing.



This indicates the break of wire at the output from the zone of deformation. Parameter ψ takes the maximum value ($\psi_{max} = 1.16$) in the same place, which means that the ductility function allows to predict not only the fracture in the deformation zone, but also outside of the die (figure 9b).

The second variant of the simulations was performed for a smaller elongation factor (1.18). In this case also fracture in drawn wire is predicted ($\psi_{max} = 1.01$), but the location of ψ_{max} is in the axis of drawn wire in the deformation zone.

In the third version of simulation the speed of wire drawing was lowered. This led to an increase in the temperature of metal and consequently, the amount of critical deformation. As a result $\psi_{max} = 0.86$ and the fracture of metal did not occur.

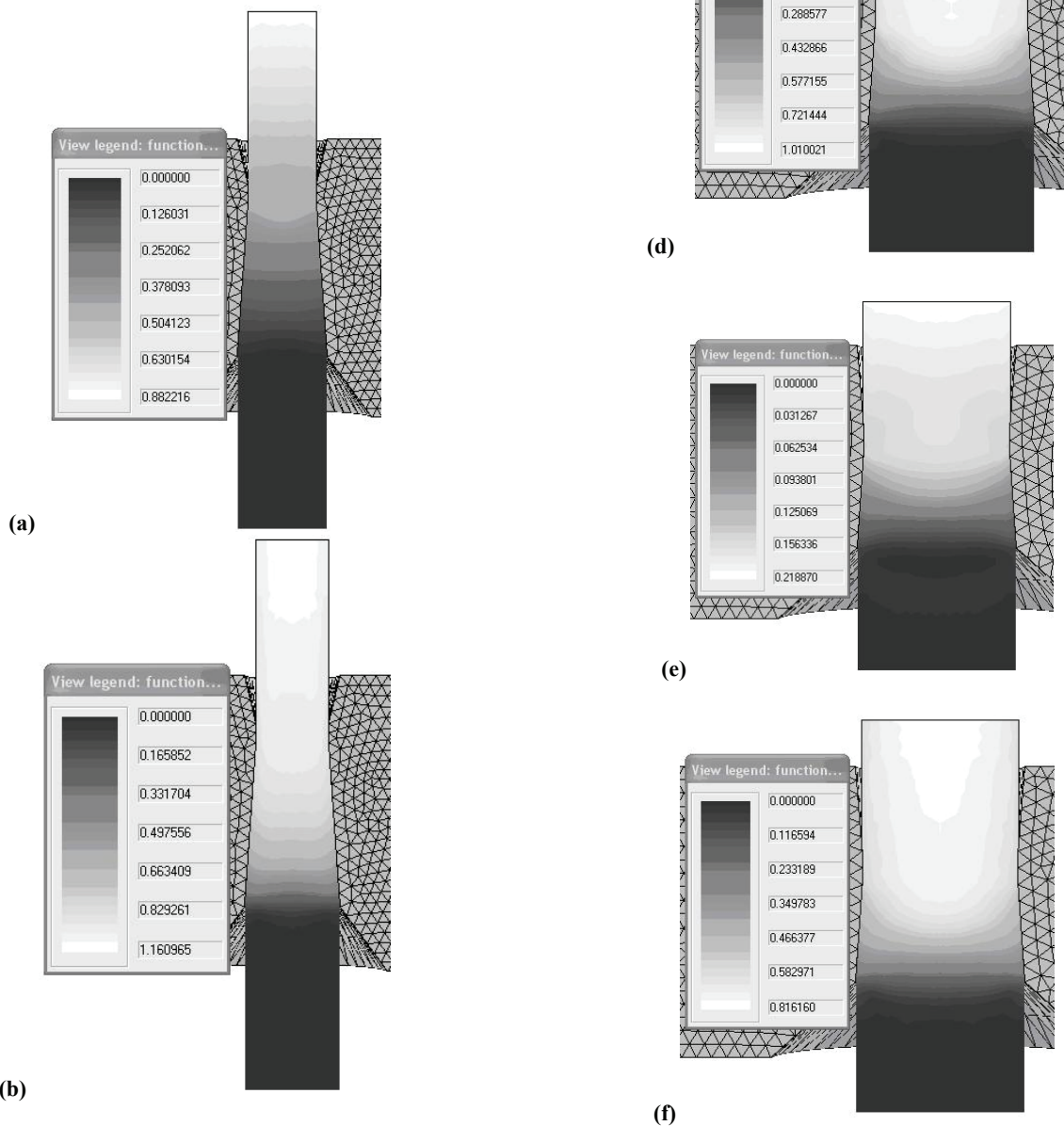


Fig. 9. Results of simulation: (a), (c), (e) – distribution of effective strain, (b), (d), (f) – distribution of ψ parameters for simulations variant 1: (a), (b); variant 2: (c), (d); variant 3: (e), (f).



9. CONCLUSIONS

Studies dedicated to the fracture of material at different values of temperature, strain rate and the triaxiality factors showed that the ductility of MgCa0.8 magnesium alloy is strongly dependent on temperature and strain rate. Therefore, the developed yield stress models and ductility functions take into account the border effect of strain rate and the temperature. Research performed for the upsetting tests and the inverse method were helpful to determine the coefficients of the yield stress model. Studies for the upsetting and tensile tests were used to calculate the coefficients of ductility function. The developed yield stress model and ductility function were implemented into the Drawing2d software.

Additionally, the analysis shows that:

1. The FE model of magnesium alloy MgCa0.8 wire drawing process, model of yield stress and ductility model in the temperature range 20 - 300°C were developed.
2. Experimental - theoretical methodology to calculate the parameters of empirical yield stress and ductility models of MgCa0.8 magnesium alloy was developed.
3. Following the developed methodology the experimental studies were performed, which are necessary to obtain the parameters of the yield stress and ductility models of the material.
4. The FE simulations show examples of different mechanisms of material fracture during drawing: break of the wire at the exit from the zone of deformation and exhaustion of the plasticity of the material deformation in the zone of deformation.

ACKNOWLEDGMENTS

The authors would like to thank the Ministry of Science and Higher Education of Poland, project no. 416/N-DFG-SFB/2009/0.

REFERENCES

- Bach Fr.-W., Milenin A., Kucharski R., Bormann D., Kustra P., 2007, Modelowanie za pomocą MES procesu ciągnięcia drutów ze stopu magnezu wykorzystywanych w chirurgii, *Hutnik-Wiadomości Hutnicze*, 74, 8-11 (in Polish).
- Bach F.-W., Kucharski R., Bormann D., 2006, Magnesium compound structures for the treatment of bone defects, *Engineering of Biomaterials*, 56-57, 58-61.
- Bach Fr.-W., Hassel T., Golovko A.N., 2005, The influence of the chemical composition and extrusion parameters on the mechanical properties of thin-walled tubes made of magnesium-calcium alloys, *Suczasi ni problemy metalurgii, Naukovi visti*, 8, Systemni technologii, 379-384.
- Eickemeyer J., Guth A., Falter M., Opitz R., 2004, Drawing of magnesium wires at Ambient temperature, *Proc. 6th Int. Conf., Magnesium alloys and their Applications*, WILEY-VCH, 318 – 323.
- Haferkamp, H., Kaese, V., Niemeyer, M., Phillip, K., Phan-Tan, T., Heublein, B., Rohde, R., 2001, *Exploration of Magnesium Alloys as New Material for Implantation*; Mat-wiss. u. Werkstofftech, 32: Wiley-VCH Verlag GmbH, Weinheim, 116-120.
- Heublein, B., Rohde, R., Niemeyer, M., Kaese, V., Hartung, W., Röcken, C., Hausdorf, G., Haverich A., 1999, Degradation of magnesium alloys: A new principle in cardiovascular implant technology, Paper TCT-69, 11. Annual Symposium Transcatheter Cardiovascular Therapeutics, *The American Journal of Cardiology*, Excerpta Media Inc., New York.
- Milenin, A., 2005, Program komputerowy Drawing2d – narzędzie do analizy procesów technologicznych ciągnięcia wielostopniowego, *Hutnik-Wiadomości Hutnicze*, 72, 100-104 (in Polish).
- Milenin, A., Kustra, P., 2008, The multiscale FEM simulation of wire fracture phenomena during drawing of Mg alloy, *Steel Research International*, 79, spec. issue Conf. Metal Forming, 1, 717-722.
- Ogawa, N., Shiomi, M., Osakada, K., 2002, Forming limit of magnesium alloy at elevated temperatures for precision forming. *International Journal of Machine Tools & Manufacture*, 42, 607-614.
- Swiostek, J., Goken, J., Letzig, D., Kainer, K.U., 2006, Hydrostatic extrusion of commercial magnesium alloys at 100°C and its influence on grain refinement and mechanical properties, *Materials Science and Engineering A*, 424, 223-229.
- Szeliga, D., Pietrzyk, M., 2007, Testing of the inverse software for identification of rheological models of materials subjected to plastic deformation, *Archives of Civil and Mechanical Engineering*, 7, 1, 35-52.
- Thomann, M., Krause, C., Bormann, D., Von der Höh N., Windhagen, H., Meyer-Lindenberg, A., 2008, Biomaterials comparison of the resorbable magnesium alloys LAE442 and MgCa0,8 concerning their mechanical properties, gradient of degradation and bone-implant-contact after 12 month implantation in rabbit model, *NRW - Fundamentals and Clinical Applications*, 3, 107-108.
- Von Mises, R., 1928, Mechanik der Plastischen Formänderung von Kristallen, *Z. Angew. Math. Mech.*, 8, 161.
- Wan, Y., Xiong, G., Luo, H., He, F., Huang, Y., Zhou, X., 2008, Preparation and characterization of a new biomedical magnesium-calcium alloy, *Materials and Design*, 29, 2034-2037.
- Watanebe, H., Mukai, T., Ishikawa, K., 2004, Different speed rolling of AZ31 magnesium alloy and the resulting mechanical properties, *Journal of Materials Science*, 39, 1477-1480.
- Cheng, Y. Q., Chen, Z. H., Xia, W. J., 2007, Drawability of AZ31 magnesium alloy sheet produced by equal channel angular rolling at room temperature, *Materials Characterization*, 58, 617–622.
- Yoshida, K., 2004, Cold drawing of magnesium alloy wire and fabrication of microscrews. *Steel Grips*, 2, 199-202.



**MATEMATYCZNY MODEL CIĄNIENIA NA
CIEPŁO STOPU MGCA0.8 UWZGLĘDNIAJĄCY
PLASTYCZNOŚĆ MATERIAŁU**

Streszczenie

W niniejszej pracy przedstawiono wyniki badań stopu magnezu MgCa0.8. Bazując na wynikach eksperymentu opracowano modeli naprężenia uplastyczniającego oraz utraty spójności materiału w zależności od prędkości odkształcenia i temperatury. Eksperyment wykonano na maszynie wytrzymałościowej Zwick Z250. Do analizy wyników wykorzystano metodę inverse. Modele numeryczne testów na spęczanie i rozciąganie pomogły w określeniu warunków utraty spójności analizowanego materiału. Opracowane modele materiału zaimplementowano do autorskiego oprogramowania Drawing2d bazującego na metodzie elementów skończonych. Takie podejście pozwoli na analizę procesu ciągnięcia w podgrzewanych ciągnadłach z uwzględnieniem kryterium utraty spójności materiału.

Received: March 31, 2010

Received in a revised form: May 8, 2010

Accepted: May 17, 2010

